AB interface in rotating superfluid ^{3}He: The first example of a superfluid shear-flow instability

R. Blaauwgeers [a,b,1], V.B. Eltsov [a,c], G. Eska [a,d], A.P. Finne [a], R.P. Haley [a,e], M. Krusius [a], L. Skrbek [a,f], G.E. Volovik [a,g]

[a] *Low Temperature Laboratory, Helsinki University of Technology, P.O. Box 2200, 02015 HUT, Finland*
[b] *Kamerlingh Onnes Laboratory, Leiden University, P.O. Box 9504, 2300 RA Leiden, The Netherlands*
[c] *Kapitza Institute for Physical Problems, Kosygina 2, Moscow 177334, Russia*
[d] *Physikalisches Institut, Universität Bayreuth, D-95440 Bayreuth, Germany*
[e] *Department of Physics, Lancaster University, Lancaster LA1 4YB, UK*
[f] *Joint Low Temperature Laboratory, Institute of Physics ACSR and Charles University, 180 00 Prague, Czech Republic*
[g] *Landau Institute for Theoretical Physics, Kosygina 2, Moscow 177334, Russia*

Abstract

The classic Kelvin-Helmholtz instability takes place on the interface between two horizontally stratified fluid layers which are in a state of relative shear flow with respect to each other. The problem was solved for the ideal case of inviscid and incompressible fluids in 1871 by Lord Kelvin. The first case of superfluid shear flow has been discovered in uniformly rotating superfluid ^{3}He, when the phase boundary between the A and B phases is maintained at a stable location with a magnetic barrier field. At sufficiently high rotation the AB interface undergoes an instability, in which the interface becomes corrugated in a standing-wave pattern. The deepest trough develops into a non-equilibrium process in which a few vortex loops are pulled across the interface and expand to rectilinear vortex lines. The critical velocity of this process displays the temperature and magnetic field dependencies which match the characteristics of the Kelvin-Helmholtz instability.

Key words: superfluid helium-3; shear flow; Kelvin-Helmholtz instability; AB phase boundary; quantized vortex lines

Kelvin-Helmholtz instability: Since Lord Kelvin's classic treatise [1,2] on the stability of the interface between two fluid layers in relative shear flow, the connection between the ideal description and the dissipative hydrodynamics of real fluids has been problematic. An example is a flag flapping in the wind. What is the connection between its fluttering and the Kelvin-Helmholtz instability [3,4]? The ideal non-dissipative limit and a rigorous treatment, which includes viscous losses, are based on a different set of equations and are not directly related. In a superfluid, on the other hand, flow remains inviscid until the instability takes place. Superfluids thus provide an environment for testing the interface between ideal and dissipative hydrodynamic theories. We discuss the first superfluid realization of the Kelvin-Helmholtz instability, the classic textbook problem in hydrodynamics [5].

AB interface in rotation: It has so far not been possible to create a situation with shear flow between two superfluids at sufficiently high relative velocity so that the instability is reached. The first experimentally accessible case, where the shear-flow instability can be set up in stationary conditions, is superfluid ^{3}He. Two of its properties are the most vital preconditions for the experiment to become possible:

1) Superfluid ^{3}He is so far the only known coherent macroscopic quantum system where a first order interface between two states (A and B) of the same order-

[1] E-mail: rob@boojum.hut.fi

parameter manifold exists. This means that the surface tension between the A and B phase is small, but also that the interface can be held at a fixed stable position. Owing to a difference in susceptibility of the two phases, the interface can be stabilized in a gradient of magnetic field.

2) There exists a remarkable difference between these two phases in the critical velocity needed to form a quantized vortex line. This difference arises from the different length scales on which vorticity forms in the A and B phases [6]. The order parameter changes symmetry and magnitude at the AB interface, but is continuous on the scale of the superfluid coherence length: $\xi \sim 10\,\mathrm{nm}$. This has far-reaching consequences on the structure of quantized vorticity: In the B phase it is the condensation energy which controls the structure of the vortex core, *ie.* within its "non-singular hard" core of radius $\sim \xi$ the magnitude of the order parameter changes. The critical velocity is high and metastable states of vortex-free superflow become possible at high velocity. In the A phase, in contrast, vortex structure is controlled by the three orders of magnitude weaker spin-orbit interaction. The "continuous" A-phase vortex has a "soft" core where only the orientation of the order parameter changes within a radius comparable to the healing length of spin-orbit coupling: $\xi_{\mathrm{D}} \sim 10\,\mu\mathrm{m}$. The continuous vortex is created at a critical velocity which is at least an order of magnitude lower than that of the non-singular vortex.

The original incentive to investigate the AB interface in rotation arose exactly from the differences in vortex structures. Vortex lines are not allowed to end at the AB interface, they either have to cross it perpendicularly or curve parallel to the interface, to form a vortex layer on the interface. But how can a continuous A-phase vortex, where the vorticity is spread over the large cross section of its soft core and which supports a circulation of two quanta, connect with the narrow-core singly quantized vortex in the B phase? Quite obviously this incompatibility in structure and quantization creates great difficulties for the interconnection of vortex lines across the interface. It was thought that a measurement of the critical velocity, the characteristic counterflow velocity of the instability at which vortex lines start to cross the interface, would provide information on the energy barrier in forming interconnections. Instead of this barrier it was found that the Kelvin-Helmholtz instability intervenes and becomes the vehicle by which interconnections are established in a complicated non-equilibrium process.

Principle of measurement: As discussed in Ref. [7], our experiment is performed in uniform rotation, by setting up a situation where the two phases slide with respect to each other along the AB interface which is oriented transverse to the rotation axis Ω. Above the interface in the A phase the number of vortex lines is

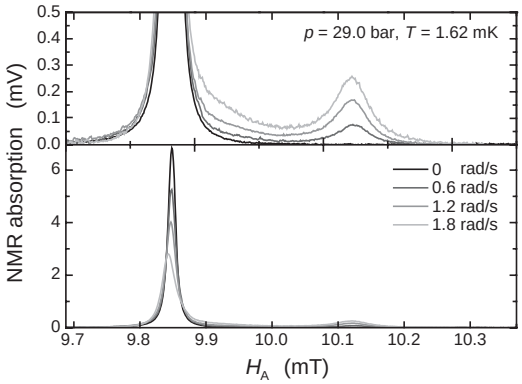

Fig. 1. NMR absorption spectra of ^{3}He-A, measured at a fixed frequency of 332 kHz as a function of magnetic field. The spectrum consists of the large bulk liquid absorption peak on the left (lower panel) which is shifted from the Larmor value, the location of the resonance line in the normal state. This temperature-dependent frequency shift has been calibrated to yield the temperature of the sample. By monitoring the frequency shift of the bulk peak the temperature can be stabilized to within one part in 10^3. The small satellite on the right (upper panel) appears only when vortex lines are formed in rotation.

at all times approaching that in the equilibrium state. This state is thus one where the superfluid is almost in solid-body rotation. Below the interface the B phase is in a state of vortex-free normal fluid - superfluid counterflow. Here the superfluid fraction is stationary in the laboratory frame.

This situation of relative shear flow is prepared by keeping all other externally controlled variables constant while the rotation velocity Ω is increased at a constant slow rate $\dot{\Omega} \sim 10^{-4}\,\mathrm{rad/s^2}$. This rate is sufficiently slow such that we can in practice consider Ω as constant. Moreover the normal fraction is so viscous that we may consider it to be always in a state of solid-body rotation. By monitoring continuously the NMR spectrum separately from the two phases one can keep track of the number of vortex lines above and below the interface. The instability is observed as a sudden event where a burst of vortex lines is introduced in the vortex-free B phase. The first event, which constitutes the threshold to a repetitive series of randomly spaced critical events, we call the onset Ω_{c}.

NMR measurement: The pick-up coils for the measurement of NMR absorption in the A and B phases are located on both sides of the AB interface, but lie far from the interface itself. The measurement of vortex lines is based on different spectral properties in the A and B phases. Fig. 1 shows a number of A-phase absorption spectra at different rotation velocities. This spectrum consists of the bulk A-phase line, which originates from the volume where the spin-orbit interaction is minimized, and from a small vortex satellite, which is generated by the spin-orbit decoupling in the soft cores. Thus the soft cores add individually to satel-

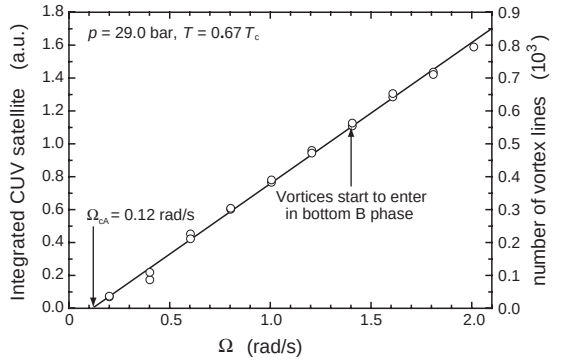

Fig. 2. Integrated intensity of the A-phase vortex satellite versus the angular rotation velocity Ω. Vortex lines contribute individually to the satellite and a linear relationship is obtained. It is used to calibrate the number of A-phase vortex lines in the sample (right vertical axis). No anomaly exists at Ω_c, the location of the shear-flow instability – this plot shows no trace of the presence of the AB interface.

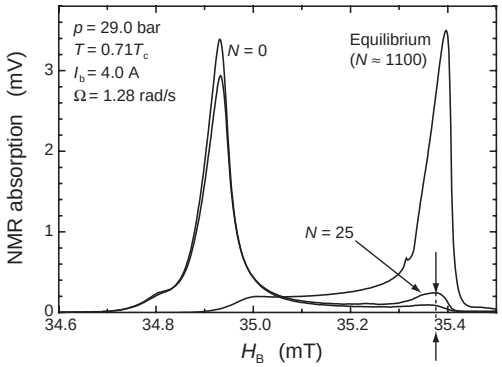

Fig. 3. NMR absorption spectra of ^{3}He-B, measured at a fixed frequency of 1.15 MHz as a function of magnetic field. In the equilibrium state, both at rest ($\Omega = 0$) and in rotation with the equilibrium number of vortex lines ($N \approx 1100$), the spectrum consists of one large asymmetric peak which borders on the right to the Larmor field value and has a long shallow temperature-dependent shoulder on the left towards low fields. In vortex-free counterflow ($N = 0$) the absorption is shifted to low fields and a new temperature-dependent maximum appears which grows sharper with increasing counterflow velocities. When vortex lines are formed ($N = 25$), the counterflow peak is reduced in height and the absorption is shifted back closer to the Larmor edge. The measurement in Fig. 4 is performed by monitoring the change in absorption with Ω at fixed field at the value of the vertical arrows.

lite absorption. The integrated intensity of the satellite is a linear function of the number of vortex lines, as shown in Fig. 2, and the zero intercept on the horizontal axis gives the critical rotation velocity Ω_{cA} where vortex formation starts. This plot is independent of the presence of the AB interface, *ie.* the same result is obtained independently whether the sample consists at this temperature of only A phase or of the two-phase configuration with the AB interface. This means that vortex formation in the A phase occurs at the outer lateral sample boundary and is not in any way connected with the AB interface [8].

In the B phase the NMR spectrum maps the order-parameter texture on the length scale of the magnetic healing length ξ_H. This length is more than an order of magnitude larger than the dipolar healing length, which defines the relevant length scale in the A phase [9]: $\xi_{H\mathrm{B}}(35\ \mathrm{mT}) \sim 0.1\,R \gg \xi_{\mathrm{D}}$ ($R = 3\,\mathrm{mm}$ is radius of our sample). Thus the NMR spectrum reflects different features in the B phase, namely the orientational distribution of the order-parameter anisotropy axis over the cross section of the sample. Its alignment is strongly deflected by macroscopic vortex-free counterflow. As illustrated by the spectra in Fig. 3, the division in absorption between the region bordering to the Larmor edge and that of the counterflow peak can be calibrated at each temperature to give the number of vortex lines. When only a small number of vortex lines is present, these are contained in a central cluster, which is coaxial with the sample cylinder and where the line density, $n_{\mathrm{v}} = 2\Omega/\kappa$, only depends on rotation velocity ($\kappa = h/(2m_3)$ is the circulation quantum). This cluster is surrounded by an annular vortex-free counterflow region which increases in width if Ω is increased and no additional vortex lines are added. This in turn increases the height of the counterflow peak. These features are employed to keep track of the number of B-phase vortex lines while the rotation velocity is slowly increased.

Measurement of AB interface instability: Fig. 4 shows a slow linear sweep of the rotation drive past the onset of the AB interface instability at constant temperature. The NMR field is tuned to a constant value close to the Larmor edge. Thus the signal decreases rapidly with increasing Ω when the absorption is shifted increasingly into the counterflow peak, until starting from the onset Ω_c it is recovered back in discontinuous jumps. These steps of random height correspond to small bursts of $1 \ldots 30$ vortex lines which are introduced in the B phase and form a central vortex cluster there. The appearance of these bursts as a function of Ω is our basic signature of the instability. The analysis of the signal in terms of the Kelvin-Helmholtz instability is presented in Ref. [10], where it is compared to the theory of the ideal inviscid case, when modified for two-fluid hydrodynamics [11]. Note that the repetitive instability events obey a linear relationship, as shown by the dashed line. This means that, although the number of vortex lines per event may vary, it occurs at a constant critical counterflow velocity $v_c = (\Omega - \Omega_c)R_{\mathrm{eff}}$. Here $R_{\mathrm{eff}} < R = 3\,\mathrm{mm}$ is the radial location of the site where the instability initially occurs and the vortices are pulled across the AB interface.

Employing the procedure in Fig. 4 the onset of the AB-interface instability can be determined as a func-

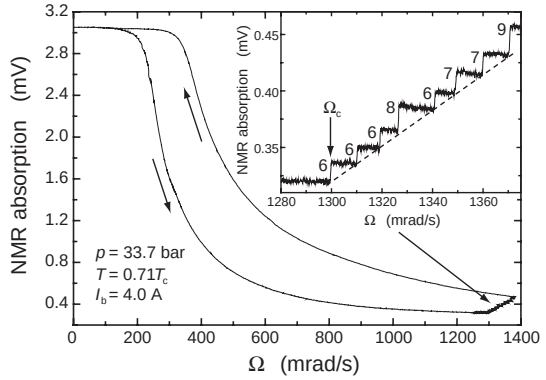

Fig. 4. B-phase NMR absorption during a slow scan of Ω from rest ($\Omega = 0$) past the onset of the AB interface instability at Ω_c and then back to rest. The absorption is measured at constant external field value close to the Larmor edge at the site of the vertical arrows in Fig. 3. The *inset* shows a magnification of the discontinuous increase in vortex lines above the onset. The staircase pattern illustrates a series of bursts in slowly increasing rotation when new vortex lines are introduced into the B phase. The number at each step gives the number of vortex lines which penetrate across the AB interface in isolated instability events.

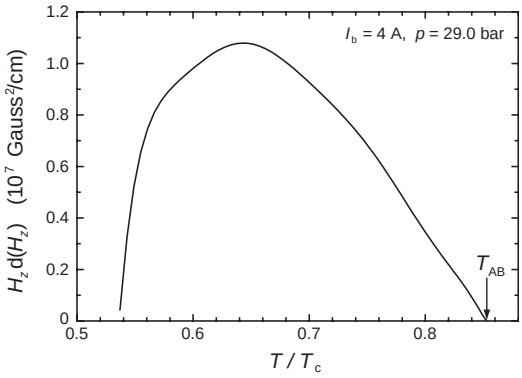

Fig. 5. Restoring force $F = (1/2)(\chi_A - \chi_B(T,H))\nabla(H_b^2)$ from the barrier field at $I_b = 4$ A on the AB interface. The temperature dependence of $F(T)$ dominates over all other terms in the AB-interface instability and therefore the curve of $\Omega_c(T)$ is of similar form.

tion of the various externally controllable parameters. Of these the most informative are the temperature dependence $\Omega_c(T)$ at constant current I_b in the barrier solenoid [10] and the current dependence $\Omega_c(I_b)$ at constant temperature [12]. Both dependences are rapidly varying functions which underline the role of the barrier field as a restoring force on the AB interface: $F = (1/2)(\chi_A - \chi_B(T,H))\nabla(H_b^2)$, where χ_A and $\chi_B(T,H)$ are the magnetic susceptibilities of the two phases. The interface resides at a height z where the field $H_b(z) = H_{AB}(T)$, *ie.* it equals the thermodynamic equilibrium field H_{AB} of the AB transition at temperature T.

The restoring force for our barrier solenoid [7] is plotted at constant current $I_b = 4$ A in Fig. 5. It has the strongest temperature dependence of all the quantities which influence the onset of the AB-interface instability. Thus a plot of $\Omega_c(T)$ resembles that of $F(T)$. On dimensional basis we can guess that this resemblance is of the simple form $v_c^4 \propto (\sigma/\rho_s^2)\,F$, where the surface tension σ and the density of the superfluid fraction ρ_s are monotonically and slowly changing functions of temperature [10].

Critical velocity of B-phase sample: The instability cannot be directly monitored at or near the AB interface with NMR measurement, owing to the highly inhomogeneous magnetic field distribution in the barrier region. What is the experimental evidence then that the step pattern in Fig. 4 really represents instability events of the AB interface rather than some other vortex formation mechanism in the B-phase section of the sample? An important aspect of the experiment is therefore the possibility to repeat the measurements under exactly the same conditions in the absence of the AB interface, *ie.* with a single-phase sample of either A or B phase. This is possible owing to the extensive supercooling of the A phase. In this way the influence of the AB interface can be identified.

It is a simple matter to check that the behavior of a single phase sample of ^{3}He-B is quite different. For this the current in the superconducting barrier solenoid is ramped to zero, the sample is cooled below the supercooled A→B transition temperature and converted into B phase. It is then warmed back to the temperature of the measurements in Fig. 4 and the same measuring procedure is repeated. In the absence of the AB interface, the first vortex lines are observed to enter at a much higher rotation velocity as an uncontrolled burst with a considerably larger number of vortex lines. In the temperature range of the present measurements of the AB-interface instability, the temperature regime of the A-phase supercooling, the critical velocity of this process is constant as a function of temperature, in contrast to the rapid and non-monotonic temperature dependence of the AB-interface instability. As analyzed in Ref. [13], the properties of the critical process in the absence of the AB interface fit the characteristics of a sudden burst of vortex lines flowing out of the orifice into the sample volume. Interesting studies can be made of the dynamics connected with this process, but here we leave these aspects aside.

For the execution of the AB-interface measurement it is thus of importance that sweeping the barrier field does not interfere with either the A or B phase NMR measurement. It can in this way also be established that in barrier fields $[H_b(z)]_{max} < H_{AB}(T)$, where the AB interface is absent, the critical velocity of vortex formation for the single phase sample of ^{3}He-B is to-

tally indifferent to I_b, as is expected for the flow of vortices through the orifice. Thus in spite of the fact that the instability cannot be directly monitored, nevertheless, many details can be inferred indirectly from the analysis of the B-phase measurements on $\Omega_c(T, I_b)$.

Characteristics of AB-interface instability: In addition to the temperature and barrier field dependences of the AB-interface instability, important properties can be extracted from a detailed analysis of the instability events in Fig. 4. The two principal conclusions are:

1) Although Ω_c is strongly temperature dependent, at constant temperature its value is reproduced accurately from one measurement to the next within the combined experimental uncertainties. This definition fits an instability.

2) From the analysis not only the radial position of the instability ($R_{\rm eff}$) can be determined, but also azimuthal information can be obtained. The number of vortices per step-like burst can be estimated as half the wavelength of the corrugation times the density of ($n = 1$) vortex lines around the periphery of the interface. This information is derived from an analysis of the distribution function of the number of vortex lines in the instability events [10] and is in agreement with the theoretical prediction. It thus provides experimental evidence for the presence of standing-wave corrugations.

This collaboration was carried out under the EU-IHP program (ULTI 3) and the ESF network COSLAB.

References

[1] Lord Kelvin (Sir William Thomson) *Mathematical and physical papers*, Vol. **4**, *Hydrodynamics and General Dynamics*, Cambridge University Press, 1910.

[2] H.L.F. von Helmholtz, Monatsberichte der königlichen Akademie der Wissenschaften zu Berlin, 215 (1868).

[3] Lord Rayleigh (J.W. Strutt), *Scientific papers*, Vol. **1**, Cambridge University Press, 1899.(Pergamon Press, Oxford, 1987).

[4] J. Zhang *et al.*, Nature **408** (2000) 835.

[5] H. Lamb, *Hydrodynamics* (Dover Publ., New York, 1932), Chap. IX; S. Chandrasekhar, *Hydrodynamic and Hydromagnetic Stability* (Dover Publ., New York, 1981), Chap. XI; L.D. Landau and E.M. Lifshitz, *Fluid Mechanics* (Pergamon Press, 1989), Chap. VII.

[6] Ü. Parts *et al.*, Europhys. Lett. **31** (1995) 449; J. Low Temp. Phys. **10**7 (1997) 93.

[7] R. Blaauwgeers *et al.*, these proceedings.

[8] R. Blaauwgeers *et al.*, Nature **404** (2000) 471.

[9] P.J. Hakonen *et al.*, J. Low Temp. Phys. **76** (1989) 225.

[10] R. Blaauwgeers *et al.*, preprint arXiv:cond-mat/0111343.

[11] G.E. Volovik, Pis'ma ZhETF **75** (2002) 491.

[12] V.B. Eltsov *et al.*, these proceedings.

[13] L. Skrbek *et al.*, these proceedings.